APPLIED AND ENVIRONMENTAL MICROBIOLOGY, June 1999, p. 2418–2428 Vol. 65, No. 6
0099-2240/99/$04.00+0

A Morphological and Molecular Perspective of *Trichoderma viride*: Is It One or Two Species?

ELKE LIECKFELDT,[1]* GARY J. SAMUELS,[2] HELGARD I. NIRENBERG,[3] AND ORLANDO PETRINI[4]

Institut für Biologie/Genetik, Humboldt-Universität, D-10115 Berlin,[1] and Institut für Pflanzenvirologie, Mikrobiologie und Biologische Sicherheit, Biologische Bundesanstalt für Land-und Forstwirtschaft, D-14195 Berlin,[3] Germany; Systematic Botany and Mycology Laboratory, Agricultural Research Service, United States Department of Agriculture, Beltsville, Maryland 20705-2350[2]; and Tera d'Sott 5, S-6949 Comano, Switzerland[4]

Received 7 December 1998/Accepted 5 April 1999

***Trichoderma* (*Ascomycetes*, *Hypocreales*) strains that have warted conidia are traditionally identified as *T. viride*, the type species of *Trichoderma*. However, two morphologically distinct types of conidial warts (I and II) have been found. Because each type corresponds to a unique mitochondrial DNA pattern, it has been questioned whether *T. viride* comprises more than one species. Combined molecular data (sequences of the internal transcribed spacer 1 [ITS-1] and ITS-2 regions and of part of the 28S rRNA gene along with results of restriction fragment length polymorphism analysis of the endochitinase gene and PCR fingerprinting), morphology, physiology, and colony characteristics distinguish type I and type II as different species. Type I corresponds to "true" *T. viride*, the anamorph of *Hypocrea rufa*. Type II represents a new species, *T. asperellum*, which is, in terms of molecular characteristics, close to the neotype of *T. hamatum*.**

Species of the genus *Trichoderma*, among them *T. viride*, are well known for their production of several lytic enzymes (32) and/or antibiotics (3). Strains of those species are widely used in biocontrol of soilborne plant-pathogenic fungi (see reference 38). The exact characterization and identification of strains to the species level is the first step in utilizing the full potential of fungi in specific applications. *T. viride* is one of the most commonly reported and widely distributed of all soil fungi (5), occurring in the most extreme to the most mundane of habitats. Many physiological, antifungal, and insecticidal activities have been attributed to this species (for a review, see reference 5). Unfortunately, literature published before 1969 is likely to be unreliable because the name "*Trichoderma viride*" was applied to most strains of *Trichoderma* spp. (2). Rifai (36) revised the genus *Trichoderma* and characterized *T. viride* by its warted conidia. Since 1969 all *Trichoderma* strains having globose, subglobose, or ellipsoidal warted conidia have been identified as *T. viride*. However, in 1989, Meyer and Plaskowitz (27) observed two different types of warts on conidia identified as *T. viride*, which they termed types I and II (to which we refer here). Later Meyer (28) found that the respective types of conidial ornamentation corresponded to types of specific mitochondrial DNA, and he suggested that two species were involved but did not propose a taxonomy.

Owing to the fact that the name *T. viride* is applied to many strains that are used in experimental or economically important applications, it is highly desirable that the name used by so many different individuals refer to a single organism. From this perspective, the suggestion by Meyer (28) that the current concept of *T. viride* comprises more than one species is unsettling. As part of our ongoing studies of *Trichoderma* systematics (9, 16, 19–23, 29, 39, 40, 47) we have used a polyphasic approach to test Meyer's two-species hypothesis. In the present work, we report on the application of combined molecular (sequences of the internal transcribed space 1 [ITS-1] and ITS-2 regions and of part of the 28S rRNA gene, along with restriction fragment length polymorphism [RFLP] analysis of the endochitinase gene and PCR fingerprinting), morphometric, and physiological approaches in a study of *T. viride*. The mixed-type data sets combining information from morphological, physiological, and molecular studies were used in a correspondence analysis (CA) (10, 44) to explore the taxonomic interrelationships within what has been called *T. viride*.

* Corresponding author. Mailing address: Institut für Biologie/Genetik, Humboldt-Universität, Chauseestr. 117, D-10115 Berlin, Germany. Phone: 49 30 2093 8143. Fax: 49 30 2093 8141. E-mail: Elke=Lieckfeldt@biologie.hu-berlin.de.

MATERIALS AND METHODS

Fungal cultures. In the present study, we included all of the strains that were previously studied by Meyer (28), additional strains of *T. viride*, anamorphs of *Hypocrea* collections that could be determined as *T. viride*, and—for preliminary observations with respect to the position of *T. viride* in the section *Trichoderma*—also strains of *T. atroviride* and *T. koningii*. Sources and designations of the 71 investigated strains are listed in Table 1. All strains were cultivated on 2% cornmeal dextrose agar (CMD; Sigma). For DNA isolation, strains were grown for 48 h in a liquid medium (19) at room temperature on a shaker (120 rpm).

Morphological studies. All measurements of anamorph characteristics were taken on cultures grown on CMD for about 1 week at 20 to 22°C. Conidiophores and conidia were measured in 3% KOH or water; KOH was used first in all cases to aid in wetting the conidia. Measurements of teleomorph characteristics were taken on herbarium material that was rehydrated briefly in 3% KOH. When possible, 30 measurements of each parameter in each collection were made.

With the permission of the director of Persoon's Herbarium (Leiden, The Netherlands), we studied conidial ornamentation in the 200-year-old lectotype collection of *T. viride* (specimen number 910 263 877 [33]), using scanning electron microscopy (SEM) and light microscopy.

We determined growth rates and colony characteristics at 20, 25, 30, and 35°C on potato dextrose agar (PDA; Difco) and on synthetic low-nutrient agar (SNA) (31). Data were obtained as described by Lieckfeldt et al. (24).

Material for SEM studies was obtained from cultures that were grown on PDA for 2 weeks at 20°C. Agar blocks with abundant conidia were prepared for SEM according to the method of Meyer and Plaskowitz (27). Specimens were examined with a JEOL T300 scanning electron microscope.

DNA isolation and PCR fingerprinting. PCR fingerprinting, RFLP analysis of the endochitinase gene, and sequencing of the ITS regions of the nuclear rRNA gene (rDNA) cluster of *Trichoderma* and *Hypocrea* strains were undertaken. DNA isolation and PCR fingerprinting were carried out as specified by Kuhls et al. (19) with a slight modification of the reaction volume of the PCR assay that amounted to only 25 μl. As primers, the sequence $(GACA)_4$ and phage M13 core sequence 5′-GAGGGTGGCGGTTCT were used.

rDNA amplification and sequencing of the rDNA fragments. Fragments containing (i) ITS-1, the 5.8S rDNA, and ITS-2 or (ii) the first part of the 28S rRNA gene, including the variable domains D1 and D2 (13), were amplified in a 100-μl-volume reaction as described by Kuhls et al. (21). Parts of the conserved regions of the small-subunit rDNA (primer SR6R [5′-AAGTAGAAGTCGTAAC

TABLE 1. List of strains investigated in this study, including EMBL and GenBank accession numbers for ITS sequences and taxon labels used in UPGMA and CA

Strain or species	Culture collection no.	Origin	EMBL/GenBank accession no. (ITS; 28S)	Taxon label in CA
T. viride (lectotype)	910-263-877[c]	Germany (?), wood		
T. hamatum	DAOM 167057	Canada, soil	ITS, Z48816; 28S, AF127151	Ha
T. viride[a]	Tr 48 = NRRL 5242	United States, lab strain	ITS, AJ230669; 28S, AF127145	Na1[d]
T. viride[a]	Tr 31	United States, lab strain	ITS, AJ230669	Na2[d]
T. viride[a]	Tr 32	Korea, soil	ITS, AJ230669	Na3[d]
T. viride[a]	Tr 50	N.C.	ITS, AJ230669	Na4[d]
T. viride[a]	GJS 90-14	Vietnam	ITS, AJ230669	Na5[d]
T. viride[a]	GJS 91-1	South Africa	ITS, AJ230669	Na6[d]
T. viride[a]	BBA 68646R	Germany, compost	ITS, AJ230680	Nb1
T. viride[a]	Tr 3 = CBS 433.97 = BBA 70684	Md., *Sclerotinia* sp.	ITS, AJ230668; 28S, AF127153	Nb2[d]
T. viride[a]	Tr 7	United States, lab strain	ITS, AJ230668	Nb3[d]
T. viride[a]	Tr 13	Md., mutant of Tr 3	ITS, AJ230668	Nb4[d]
T. viride[a]	Tr 44	Ga., soil	ITS, AJ230668	Nb5[d]
H. vinosa	GJS 94-81	New Zealand, *Hoheria* sp.	ITS, AJ230668	Nb6[d]
T. viride[a]	BBA 68543	Germany, *Dieffenbachia* sp.	ITS, AJ230668	Nb7
T. viride[a]	GJS 91-160	Brazil, soil	ITS, AJ230668	Nb8[d]
T. viride[a]	GJS 90-7	Vietnam	ITS, AJ230668	Nb9[d]
T. viride[a]	GJS 91-162	Brazil, soil	ITS, AJ230668	Nb10[d]
T. viride[a]	GJS 91-24	?	ITS, AJ230668	Nb11[d]
H. spec.	Hy 42	Wash.	ITS, X93982	At1
T. atroviride	DAOM 165779	N.C.	ITS, Z48817; 28S, AF127151	At2
Hypocrea sp. cf. *rufa*	GJS 96-200	Costa Rica	ITS, AJ230659	At3[d]
H. muroiana	GJS 97-26	Japan, *Quercus* sp. with *Lentinus edodes*	ITS, AJ230659	At4[d]
H. rufa	GJS 90-134	Ga., decorticated wood	ITS, AJ230659	At5[d]
H. rufa	Hy 5	Ind.	ITS, AJ230659	At6[d]
T. atroviride	BBA 68768	Germany, compost	ITS, AJ230659	At7
T. atroviride	BBA 68600	Germany, compost	ITS, AJ230659	At8
T. atroviride	BBA 68601	Germany, compost	ITS, AJ230659	At9
T. atroviride	BBA 70227	Denmark, wet carpet	ITS, AJ230659	At10
T. atroviride	BBA 70228	Denmark, wet carpet	ITS, AJ230659	At11
T. atroviride	BBA 65348R	Sweden, conifer	ITS, AJ230659	At12
T. viride[b]	Tr 8 = WSF 2023	Wis., soil	ITS, X93986	Vb1[d]
T. viride[b]	Tr 2 = ATCC 18652	Colombia, soil	ITS, X93978; 28S, AF127150	Vb2[d]
T. viride[b]	Tr 22 = ATCC 28020	Wash., soil	ITS, AJ230678	Vb3[d]
T. viride[b]	GJS 91-62	Va., *Acer* wood	ITS, AJ230678	Vb4[d]
T. viride[b]	BBA 70238	Germany, turf	ITS, AJ230678	Vb5
H. rufa	Hy 70	New Zealand, *Fomes* sp.	ITS, AJ230678	Vb6[d]
T. viride[b]	GJS 92-14	New Zealand, pine	ITS, AJ230678	Vb7[d]
T. viride[b]	GJS 92-15	Canada, peat	ITS, AJ230678	Vb8[d]
Hypocrea sp. cf. *rufa*	GJS 89-127	N.C., Indet tree	ITS, X93980	Vb9[d]
T. viride[b]	Tr 21 = ATCC 28038	Va., soil	ITS, AJ230675	Vb10[d]
T. viride[b]	GJS 90-95	N.C., decorticated wood		
H. vinosa	GJS 94-9	Taiwan, bark	ITS, AJ230670	Ko1[d]
H. vinosa	GJS 94-10	Taiwan, bark	ITS, AJ230671	Ko2[d]
H. vinosa	GJS 94-11	Taiwan, bark	ITS, AJ230671	Ko3[d]
T. koningii	ATCC 64262	Hungary	ITS, Z79628; 28S, AF127149	Ko4
T. koningii	CBS 457.96 = GJS 96-117	The Netherlands, soil	ITS, Z79628	
T. koningii	CBS 458.96 = GJS 96-118	The Netherlands, soil	ITS, Z79628	Ko5[d]
T. koningii	CBS 459.96 = GJS 96-120	The Netherlands, soil	ITS, Z79628	
T. koningii	CBS 460.96 = GJS 96-119	The Netherlands, soil	ITS, Z79628	
T. koningii	GJS 89-122	Md., wood	ITS, Z79628	Ko6[d]
H. rufa	GJS 97-243	Ga., oak wood	ITS, AJ230667	Ko7[d]
H. rufa	GJS 96-47	Puerto Rico, wood	ITS, AJ230685	Ko8[d]
T. atroviride	DAOM 165782	N.C.	ITS, Z48818	Ko9
T. koningii	GJS 90-18	Wis., burned wood		
Trichoderma sp. cf. *viride*[b]	BBA 68432	Russia/Petrograd, wheat	ITS, AJ230686	Vd1
Trichoderma sp. cf. *viride*[b]	BBA 70470	Germany, wet building	ITS, AJ230682	Vd2
T. viride[b]	GJS 92-11	New Zealand, pine	ITS, AJ230682	Vd3[d]
Hypocrea sp. cf. *rufa*	GJS 89-142	N.C., decorticated log	ITS, X93987	Vd4[d]
H. rufa	GJS 94-118	France, bark	ITS, AJ230679	Vd5[d]
T. viride[b]	Tr 4	Oreg., roots of Douglas fir infected with *Phellinus weirii*	ITS, AJ230682	Vd6[d]
T. viride[b]	Tr 5	Oreg., see Tr4	ITS, AJ230682	Vd7[d]

Continued on following page

TABLE 1—*Continued*

Strain or species	Culture collection no.	Origin	EMBL/GenBank accession no. (ITS; 28S)	Taxon label in CA
T. viride[b]	Tr 6	Oreg., see Tr4	ITS, AJ230682; 28S, AF127147	Vd8[d]
T. viride[b]	Tr 26 = ATCC 32630	Sweden, beach wood	ITS, AJ230682	Vd9[d]
Trichoderma sp. cf. *viride*[b]	BBA 66069R	Germany, soil	ITS, AJ230681	Vd10[d]
Trichoderma sp. cf. *viride*[b]	BBA 65450	Germany, soil	ITS, AJ230673	Vd11[d]
Trichoderma sp. cf. *viride*[b]	BBA 70471	?	ITS, AJ230682	Vd12
H. vinosa	GJS 96-163	Taiwan, wood	ITS, AJ230672	Ve1[d]
H. rufa	Hy 9	Fla., wood	ITS, AJ230674; 28S, AF127146	Ve2
T. viride	GJS 90-20	Wis., wood	ITS, AJ230676	Ve3[d]
H. rufa	GJS 90-125	N.C., oak wood	ITS, AJ230677	Ve4[d]

[a] All strains are *T. viride* type II (27) and represent the new species *T. asperellum* (41).
[b] All strains are *T. viride* type I (27) and represent true *T. viride*.
[c] Persoon L0018559 type, Rijksherbarium, Leiden, The Netherlands.
[d] All strains that are included in the CA.

AAGG]) and the large-subunit rDNA (primers LR1 [5′-GGTTGGTTTCTTTT CCT], LR7 [5′-TACTACCACCAAGATCT], and LROR [5′-ACCCGCTGAA CTTAAGC]) flanking the ITSs were used as primers (49). For direct cycle sequencing, fragments were purified (QIAquick PCR purification kit; Qiagen). The sequencing was done with an automatic sequencer (model A373; Applied Biosystems). Both DNA strands were sequenced, and reactions were carried out with a BigDye Terminator Cycle Sequencing Kit (Applied Biosystems), using 50 ng of purified PCR fragments and 10 pmol of the respective primer (SR6R, 5.8S, 5.8SR, LR1, or LR3 [49]). Cycle sequencing was performed in a DNA engine (MJ Research) programmed for 50 cycles of 30 s at 95°C, 20 s at 50°C, and 4 min at 60°C after an initial step of 1 min at 95°C. The assay reaction mixture had a volume of 10 μl. Surplus dye terminators were removed by sodium acetate-ethanol precipitation of the DNA.

The 28S rDNA fragments amplified with the primer pair LROR and LR7 were also used for RFLP analysis with the restriction enzymes *Hae*III, *Hha*I, *Msp*I, and *Sau*96I. The assay followed exactly the conditions described for the RFLP analysis of the endochitinase gene (see below).

PCR amplification and RFLP analysis of the 42-kDa endochitinase gene. PCRs were performed with the oligonucleotides 5′-CACTTCACCATGTTGG GCTTCCTC and 5′-GATCTCTAGTTGAGACCGCTTCGG as primers (6). The 50-μl reaction volume contained 25 ng of genomic DNA and 0.2 μM each respective primer. The amplification program included an initial denaturation for 4 min at 94°C; 35 cycles of 30 s at 94°C, 1 min at 60°C, and 1 min at 72°C; and a final extension step of 10 min at 72°C. Amplification products from 5 μl of the assay reaction mixture were first checked by electrophoresis in a 1.2% agarose gel buffered with 1× Tris-borate-EDTA (37). For those strains that exhibited two endochitinase gene fragments, the 1.4-kb fragment was purified from the agarose gel by using a Jetsorb purification kit (Genomed, Bad Oeynhausen, Germany) according to the protocol provided by the supplier. For RFLP analysis, 15 μl of the amplification product was completely digested with 12 U of restriction enzyme (*Hae*III, *Hha*I, *Msp*I, or *Sau*96I) at 37°C according to the manufacturer's (New England Biolabs) instructions. Digested DNA was electrophoresed in 2.0% agarose gels for 5 h at 110 V in 1× Tris-borate-EDTA buffer.

Data analysis. For RFLP data, the presence or absence of bands was coded in binary form (0/1) and the matrix was used in both parsimony analysis (PAUP 3.1.1) (46) and cluster analysis with the UPGMA algorithm (Treecon) (48).

The PCR fingerprint patterns of the groups that were revealed by the other molecular methods were compared visually only.

The analysis of sequence data was performed with the PAUP 3.1.1 software after an initial alignment of the nucleotide sequences comprising the entire 650-bp sequence determined with the multiple-alignment program CLUSTAL V, using visual optimization when needed. (Sequence alignments are available upon request.) Parsimony analysis was carried out in two steps. A first analysis included all of the sequences and was performed with the heuristic search option of PAUP 3.1.1 (data not shown). The second search was done on a subset of 10 sequences, representing the main sequence types, by using the branch-and-bound algorithm with single gaps treated as a fifth base. In both analyses, *T. longibrachiatum* (Z31019) and *T. polysporum* (Z48815) were used as outgroups. Bootstrap analysis with 1,000 replications was done to test the robustness of the internal branches (7) of the single-most-parsimonious tree that was found in the branch-and-bound analysis.

Exploratory data analysis was carried out on the morphological data, using either analysis of variance or nonparametric tests when appropriate, and included box plot displays, growth curves, and statistical testing. Exploratory analysis and statistical tests were performed with the software package Systat 6.0 (51). In addition, a CA was carried out on the molecular data set as described in detail by Sieber et al. (44). Briefly, a matrix was constructed that contained all molecular data, expressed as the presence or absence (0 or 1, respectively) of a given molecular character or band. The resulting matrix was then subjected to multiple CA, using the package SimCA 2.1 (10).

To test the fitting of the data to the models, CA was also carried out on a combined matrix of the molecular and phenetic data of the individual isolates versus the species centroids (i.e., "ideal species") (for details of the method, see reference 44). The morphological and molecular characteristics were coded as detailed in Table 2, and then the codes were transformed in class variables as described by Sieber et al. (44). The resulting matrix was then subjected to multiple CA (44). Classes were formed in accordance with the method of Sieber et al. (44). A statistical approach was adopted to define classes within each variable. Means and standard deviations (SD) of the measurements of all collections were calculated. The central class was then defined as the mean ± 0.5 SD, and all other classes were subsequently 1 SD in width. For the computation of the CA shown in Fig. 2, only the data for the isolates studied by morphological and molecular methods were used as active variables, while the data for the ideal species (ATRO, KONI, TV1B, TV1D, TV1E, TV2A, and TV2B) were inserted in the CA as supplementary variables and thus did not influence the outcome of the analysis.

Nucleotide sequence accession numbers. The ITS nucleotide sequences determined in this study have been submitted to the GenBank and EMBL databases, and their accession numbers are listed in Table 1.

RESULTS

Morphology. Fifty-seven strains of *Trichoderma* and *Hypocrea* (Table 1) were characterized with respect to a total of 42 morphological and physiological characteristics (Table 2). For the Persoon collection (lectotype material), SEM of conidia was performed. Conidia from this collection were measured, and the few remaining phialides were observed.

(i) Anamorph characteristics. The most important characteristics are presented in Table 3. A more-detailed description of morphological characteristics is given elsewhere (41). Conspicuous differences in conidial shape and ornamentation, arrangement of conidiophores within conidial aggregates, branching of the conidiophores (regular or irregular), the arrangement of phialides on conidiophores, and the shape of the phialides were seen.

Three basic types of conidial ornamentation were observed by light microscopy and SEM. Some collections had conspicuous, grossly warted conidia with broadly rounded warts (*T. viride* type I [27]). Conidial warts of other collections were slightly more irregular and pyramidal (*T. viride* type II [27]). A number of collections had smooth conidia (*T. atroviride* or *T. koningii*). Conidia of Persoon specimens of *T. viride* had conspicuous, broadly rounded warts of type I.

Phialides of *T. viride* types I and II had a mean length of 9 μm or more, while those of *T. atroviride* and *T. koningii* tended to be shorter, with a median length of less than 8.5 μm. The length/width (l/w) ratio of phialides was greater than 3 for *T. viride* type I and *T. koningii* and less than 3 for *T. viride* type II and *T. atroviride*.

The median lengths and widths of the conidia of all the strains were between 3.0 and 4.5 μm and between 2.0 and 4.0 μm, respectively. The most obvious difference was in conidial

TABLE 2. Description of morphological and molecular characteristics, classes, and variables used for UPGMA and CA of the *T. viride* data set

Characteristic	Characteristic described	Class	Variable
1	Angle subtending the phialide (A)	1 = >100°	A1
		2 = <100°	A2
		3 = unknown	A3
2	Length of conidia from CMD (CL)	1 = <3.9 μm	CL1
		2 = >3.9 μm	CL2
		3 = unknown	CL3
3	Width of conidia from CMD (CW)	1 = <3.1 μm	CW1
		2 = >3.1 μm	CW2
		3 = unknown	CW3
4	Length of conidia from SNA (SL)	1 = 2.5–3.5 μm	SL1
		2 = 3.6–4.0 μm	SL2
		3 = >4.0 μm	SL3
		4 = unknown	SL4
5	Width of conidia from SNA (SW)	1 = 2.5–3.0 μm	SW1
		2 = 3.1–3.5 μm	SW2
		3 = >3.5 μm	SW3
		4 = unknown	SW4
6	Phialide length (PH)	1 = <8.2 μm	PH1
		2 = 8.2–8.5 μm	PH2
		3 = >8.5 μm	PH3
7	Phialide middle (M)	1 = 2.0 to <3.0 μm	M1
		2 = >3.0 μm	M2
8	Phialide base (B)	1 = <2.0 μm	B1
		2 = >2.0 and <2.9 μm	B2
		3 = >2.9 μm	B3
9	Hypha below phialide, axis (AX)	1 = <2.0 μm	AX1
		2 = 2.0–2.9 μm	AX2
		3 = >2.9 μm	AX3
10	Chlamydospore diameter (CY)	1 = <9.0 μm	CY1
		2 = 9–9.5 μm	CY2
		3 = >9.5 μm	CY3
		4 = unknown	CY4
11	l/w ratio of phialides (PR) from CMD	1 = <3.0	PR1
		2 = >3.0	PR2
		3 = unknown	PR3
12	l/w ratio of conidia (CR) from CMD	1 = 1.0–1.2	CR1
		2 = 1.3–1.7	CR2
		3 = unknown	CR3
13	Ascus length (AL)	1 = <85 μm	AL1
		2 = >85 μm	AL2
		3 = unknown	AL3
14	Ascus width (AW)	1 = <6.0 μm	AW1
		2 = >6.0 μm	AW2
		3 = unknown	AW3
15	Length, distal part, ascospore (DL)	1 = <4.5 μm	DL1
		2 = >4.5 μm	DL2
		3 = unknown	DL3
16	Width, distal part, ascospore (DW)	1 = <3.9 μm	DW1
		2 = >3.9 μm	DW2
		3 = unknown	DW3
17	Length, proximal part, ascospore (XL)	1 = 4.0–4.9 μm	XL1
		2 = >4.9 μm	XL2
		3 = unknown	XL3
18	Width, proximal part, ascospore (XW)	1 = <3.6 μm	XW1
		2 = >3.6 μm	XW2
		3 = unknown	XW3
19	Stromal diameter (ST)	1 = <1.5 mm	ST1
		2 = >1.5 mm	ST2
		3 = unknown	ST3
20	Perithecial height (PI)	1 = <232 μm	PI1
		2 = >232 μm	PI2
		3 = unknown	PI3
21	Perithecial width (PD)	1 = 140–170 μm	PD1
		2 = 171–180 μm	PD2
		3 = >180	PD3
		4 = unknown	PD4
22	Width of surface layer of stroma (SR)	1 = <20 μm	SR1

Continued on following page

TABLE 2—*Continued*

Characteristic	Characteristic described	Class	Variable
		2 = >20 μm	SR2
23	Diameter of surface cells of stroma seen in section (SC)	1 = 4.5–5.0 μm	SC1
		2 = >5.0 μm	SC2
		3 = unknown	SC3
24	Surface cells of stroma seen in surface view (SV)	1 = <5.0 μm	SV1
		2 = 5.0–5.5 μm	SV2
		3 = >5.5 μm	SV3
		4 = unknown	SV4
25	Cells of interior of stroma below perithecia (IN)	1 = 5.0–6.0 μm	IN1
		2 = 6.1–7.0 μm	IN2
		3 = >7.0 μm	IN3
26	Hairs on stroma surface, length (HL)	1 = <12 μm	HL1
		2 = >12 μm	HL2
		3 = unknown	HL3
27	Hairs on stroma surface, width (HW)	1 = 3.5–4.1 μm	HW1
		2 = >4.1 μm	HW2
		3 = unknown	HW3
28	Conidial shape (CT)	1 = subglobose, strongly warted	CT1
		2 = subglobose, weakly warted	CT2
		3 = subglobose, smooth	CT3
		4 = oblong to ellipsoidal, smooth	CT4
29	Presence of coconut odor (OD)	1 = absent	OD1
		2 = present	OD2
30	Formation of chlamydospores on CMD within 1 week (CH)	1 = present	CH1
		2 = absent	CH2
31	Growth on PDA at 72 h, 25°C (P25)	1 = weak growth	P251
		2 = moderate growth	P252
		3 = strong growth	P253
32	Growth on PDA at 72 h, 30°C (P30)	1 = weak growth	P301
		2 = moderate growth	P302
		3 = strong growth	P303
		4 = no growth	P304
33	Time (h) at which conidia first observed on PDA at 25°C (PF)	1 = 32 h	PF1
		2 = 40 h	PF2
		3 = 64 h	PF3
		4 = 72 h	PF4
		5 = conidia not formed	PF5
34	Time (h) at which conidia first observed on SNA at 25°C (SF)	1 = 32 h	SF1
		2 = 40 h	SF2
		3 = 64 h	SF3
		4 = 72 h	SF4
		5 = conidia not formed	SF5
35	Conidial color at 25°C on PDA (CC)	1 = green	CC1
		2 = pale green	CC2
		3 = white	CC3
		4 = conidia not formed	CC4
36	Colony reverse on PDA (PS)	1 = cream	PS1
		2 = cream and folded	PS2
		3 = none	PS3
37	Margin of colony on SNA, 10 days (SE)	1 = smooth	SE1
		2 = lobed	SE2
		3 = fringed, thick ends	SE3
		4 = fringed	SE4
		5 = loose	SE5
		6 = none	SE6
38	Colony radius on PDA, 25°C, 24 h (P3)	1 = <5 mm	P31
		2 = >5–10 mm	P32
		3 = >10–15 mm	P33
		4 = >15 mm	P34
39	Colony radius on SNA, 25°C, 48 h (S3)	1 = <5 mm	S31
		2 = <5–10 mm	S32
		3 = >10–20 mm	S33
		4 = >20–25 mm	S34
		5 = >25 mm	S35
40	Surface of aggregate on CMD (AS)	1 = conidia formed at surface; projecting, terminally fertile conidiophores conspicuous	AS1
		2 = conidia formed from plumose, projecting conidiophores that are entirely fertile	AS2

Continued on following page

TABLE 2—*Continued*

Characteristic	Characteristic described	Class	Variable
		3 = aggregates uniformly cottony with no projecting conidiophores	AS3
41	Morphology of phialides (PM)	1 = hooked and/or sinuous phialides present	PM1
		2 = phialides straight	PM2
		3 = unknown	PM3
42	Morphology of branches (BT)	1 = regular with branches tending to be paired and regularly spaced	BT1
		2 = irregular with long internodes between branches, fertile aggregate tending to be sinuous; phialides tending to be solitary	BT2
		3 = unknown	BT3
43	RAPD pattern M13 (RAPD)	Patterns 1–8	RAPD1–RAPD8
		No data	RAPD9
44	RAPD pattern $(GACA)_4$ (TYPE)	Patterns 1–8	TYPE1–TYPE8
		No data	TYPE9
45	ITS sequence type (ITS)	Types 1–8	ITS1–ITS8
46	Endochitinase gene fragment (EGF)	1 = 1 fragment	EGF1
		2 = 2 fragments	EGF2
		3 = unknown	EGF3
47	Endochitinase gene RFLP, *Hae*III (EH)	Patterns 1–12	EH1–EH12
		No data	EH13
48	Endochitinase gene RFLP, *Hha*I (HhaI)	Patterns 1–6	HhaI1–HhaI6
		No data	HhaI7
49	Endochitinase gene RFLP, *Msp*I (MspI)	Patterns 1–11	MspI1–MspI11
		No data	MspI12
50	Endochitinase gene RFLP, *Sau*96I (Sau96I)	Patterns 1–5	Sau96I1–Sau96I5
		No data	Sau96I6
51	28S sequence type (D28)	Types 1–6	D281–D286
		No data	D280
52	28S RFLP, *Hae*III (DH28)	Pattern 1	DH281
		No data	DH280
53	28S RFLP, *Hha*I (RHh)	Pattern 1	RHh1
		No data	RHh0
54	28S RFLP, *Msp*I (PM)	Pattern 1	PM1
		Pattern 2	PM2
		No data	PM0
55	28S RFLP, *Sau*96I (PS)	Pattern 1	PS1
		No data	PS0

shape, which is to some extent reflected by the l/w ratio of the conidia. Conidia of *T. koningii* are conspicuously oblong to ellipsoidal and have an l/w ratio of 1.6, whereas conidia of *T. viride* types I and II and *T. atroviride* are globose to subglobose, with l/w ratios of between 1.1 and 1.2. There is a tendency for conidia of type II to have a slightly larger l/w ratio than those of type I, and therefore many conidia of type II tend to appear ovoidal rather than subglobose.

Chlamydospores were produced within 1 week by some members of all groups but were more frequently found in *T. viride* type II than in type I; *T. koningii* and *T. atroviride* had intermediate positions.

(ii) Cultural observations. Strains of *T. viride* type II had a much higher growth rate than type I strains, *T. atroviride*, or *T. koningii*. This was especially evident at or above 30°C. At 30°C, *T. viride* type I, *T. atroviride*, and *T. koningii* colonies had radii of less than 10 mm, whereas the radii of colonies of *T. viride* type II reached nearly 30 mm within 40 h. Only strains of type II were able to grow at 35°C.

A coconut-like odor was detected for all *T. atroviride* strains and for some strains of *T. viride* types I and II but not for any of the *T. koningii* strains.

None of the colonies produced a diffusing pigment. All produced dark-green conidia (18) (28D8) on CMD within 1 week

TABLE 3. Salient phenotypic characteristics of strains of *T. viride* M type I (true *T. viride*) and type II (*T. asperellum*)

T. viride group	Characteristic					
	Conidial warts	Conidiophores	Phialides	Chlamydospores	Temp optimum	Colony radius (mm)[a]
T. viride	Conspicuous	Irregularly branched; branches usually not paired	Tending to be sigmoidal or hooked; l/w ratio, 3.3	Typically absent	25	11–33
T. asperellum	Inconspicuous	Regularly branched; branches typically paired	Straight; l/w ratio, 2.4	Typically present	30	31–47

[a] Radii of colonies on PDA after incubation at optimum temperature for 48 h.

when grown at 20°C under conditions of alternating cool white fluorescent light and darkness. There were, however, differences between *T. viride* types I and II in the speed with which conidia were formed and became green. Conidia formed in PDA cultures of *T. viride* type II strains grown at 20 or 25°C were already dark green within 40 to 48 h, whereas the type I strains and most *T. atroviride* and *T. koningii* strains grown at 20 or 25°C formed conidia very slowly, and within 40 to 48 h there were either no conidia or only a few pale-green conidia.

(iii) Teleomorph characteristics. Each of the distinct groups that we studied included strains that were derived, or were said to have been derived, from ascospores of *Hypocrea* species. Unfortunately, only one strain derived from ascospores was included in *T. viride* type II (GJS 94-81; ICMP 5411 as *Hypocrea vinosa*), but we were not able to locate a specimen from which that culture was derived (PDD) and thus cannot confirm that connection.

Stromata of all groups formed either on decorticated wood, less frequently on bark, of hardwood trees and other fungi. They were pulvinate to discoidal, 0.5 to 1.5 mm in diameter, and brown; when young, stromata tended to be slightly effused and were light tan at the periphery. The surface was velvety, especially when young, and ostiolar openings were not visible. We could not distinguish the teleomorphs of the various *Trichoderma* groups based only on their anatomy or gross morphology.

DNA data. For a total number of 65 strains, we obtained PCR fingerprinting, RFLP, and sequence data.

(i) ITS sequencing. Sequencing of the ITSs of the ribosomal gene complex revealed a total of 13 to 17 base pair differences in ITS-1 and ITS-2 sequences between *T. viride* types I and II (Fig. 1). Each of those two sequence groups included two subgroups. Conidial ornamentation type I includes ITS groups Vb and Vd, and type II includes ITS groups Na and Nb. Moreover, subgroups Vb and Vd clustered together with strains that conformed morphologically, and in their DNA characteristics as well, to *T. atroviride* (subgroup At) and *T. koningii* (subgroup Ko), respectively. In addition, there was a fifth ITS subgroup, Ve, that did not conform to any described *Trichoderma* species. Ve was basal to the cluster including Vb, Vd, At, and Ko (Fig. 1). Sequence variation among the subgroups was found to be generally very low. For example, Na and Nb differed in 1 bp each in ITS-1 and ITS-2. Interestingly, there was also little sequence variation (ITS-1, 1 or 2 bp; ITS-2, 2 to 5 bp) among *T. viride* type I subgroups Vb and Vd, *T. atroviride* (At), and *T. koningii* (Ko). The only exception was subgroup Ve, which showed sequence differences from all other subgroups that were in the same range (12 to 17 bp) as was found for the main groups of types I and II. This was due to a greater within-subgroup sequence variation in Ve. In the parsimony tree (Fig. 1), *T. viride* type I (Vb and Vd), Ve, At, and Ko form one clade whereas *T. viride* type II (Na and Nb) forms a second clade, both supported by high bootstrap values. The separation of subgroups in this tree is not so clear. Notable is the position of the ex neotype strain of *T. hamatum* as a sister clade of the clade including the type II strains of *T. viride*.

An attempt, done with permission, to isolate DNA from the lectotype specimen of *T. viride* was not successful.

(ii) 28S RFLPs and sequencing. For a total of 20 strains, representing all seven ITS subgroups, a 569-bp part of the 5′ end of the 28S rDNA spanning the variable domains D1 and D2 (13) was first analyzed by RFLP with four restriction enzymes and then sequenced. Although the base pair differences in D1 and D2 in general were less numerous than those found in the ITS regions, the same groups and subgroups were resolved in a PAUP tree (data not shown) (alignments are available upon request).

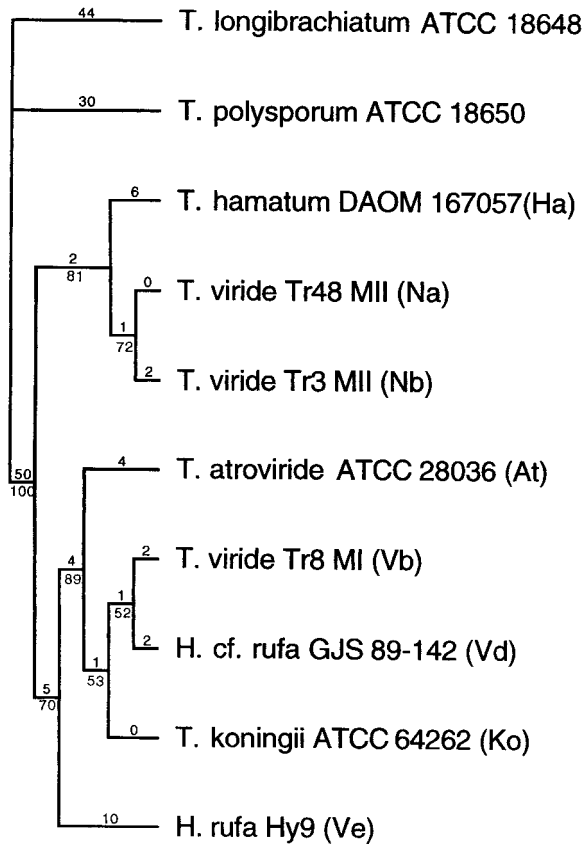

FIG. 1. Phylogenetic relationships among subgroups of *T. viride*. The cladogram is the single most parsimonious tree inferred by parsimony analysis based on rDNA sequences, including the ITS-1, 5.8S, and ITS-2 regions, using the branch-and-bound algorithm of PAUP 3.1.1 (164 steps, CI = 0.951; RI = 0.896; RC = 0.852). *T. longibrachiatum* and *T. polysporum* were used as outgroups. The numbers below the branches indicate the percentage at which a given branch was supported in 1,000 bootstrap replications. The total number of nucleotide changes assigned to each branch is shown above the branch.

(iii) PCR fingerprinting. PCR fingerprinting with two different primers gave patterns that distinguished *T. viride* type I strains from those of type II. Moreover, the patterns show intragroup variation reflecting the subgroups defined by ITS sequence variation in both groups (data not shown).

(iv) The 42-kDa endochitinase gene. PCR amplification of the 42-kDa endochitinase gene resulted in a product of the expected size (1,450 bp) for all investigated strains. Strikingly, there was an additional reproducible fragment (900 bp) in all 11 strains of ITS subgroup Nb. The 900-bp fragment was also present in strain Na3 (the second subgroup of type II). RFLP analysis of the 1,450-bp fragment revealed 5 to 12 patterns for the four enzymes used. The calculated 1/0 data for all enzymes were combined and used in parsimony as well as cluster analysis of 20 strains representing all ITS subgroups. The trees resulting from both analyses yielded essentially the same results as did ITS sequences (data not shown). There was a clear separation of *T. viride* types I and II into two clusters with a distance value of more than 0.6 between them (UPGMA analysis). RFLP analysis of the endochitinase gene revealed the same subgroups of types I and II as were revealed by ITS sequencing. However, one of the strains that was placed in subgroup Ve (Ve3 = GJS 90-20) by ITS sequencing was placed

in Vb by the endochitinase analysis. Although Ve is morphologically and genetically diverse, strain Ve3 is morphologically consistent with *T. viride* type I.

Combined data analysis. (i) CA of molecular data. The result of a simple CA performed on the weighted matrix of molecular data, including the information from ITS and 28S rDNA sequencing, PCR fingerprinting, and RFLP analysis of the endochitinase gene, revealed a good discrimination of the two subgroups Na and Nb of *T. viride* type II on the first axis. All other isolates, representing *T. viride* type I, *T. atroviride*, and *T. koningii*, were not separated by the numerical analysis (data not shown).

(ii) CA of combined morphological and molecular data. The results of the analysis using both morphological and molecular data are detailed in Fig. 2. The analysis was carried out on a standardized data matrix that included 13 molecular and 42 morphological characteristics. For each of the characteristics we defined classes, resulting in a total of 217 classes, which are described in Table 2. To minimize the influence of missing data, CA of combined data was carried out on 47 strains only (indicated in Table 1). The inertia explained by the first four factors was approximately 38% for this analysis and shows a good fit of the data to the model. In Fig. 2a, the positions of all isolates studied and of the ideal species (as constructed by using the results of the original analysis) are shown. All isolates belonging to one of the two subgroups of *T. viride* type II (Na or Nb) group closely to the ideal species TV2A and TV2B (as defined for *T. viride* type II) and are clearly separated from all other entities (discrimination on the first axis). The morphological data, however, do not distinguish the two groups that were discriminated in the molecular analysis, as can be seen from the compact group that they form. On the other hand, the other entities that could not be separated very clearly by molecular data seem to be more clearly separated according to morphological data in this analysis. Strains of subgroups At and Ko are no longer included in the big group that comprises Vb and Vd but form one group together with two isolates of Ve. This group also includes the ideal species ATRO, KONI, and TV1E (as defined for *T. atroviride*, *T. koningii*, and an as-yet-unnamed group of *Hypocrea* and *Trichoderma* collections that showed similarities to *T. viride* [Fig. 2a]). A few isolates of the group (Ko1, Ko2, and Ko3) have a more isolated position in the graph and could be considered distinct from all other isolates of this group. Isolates At4, Ko7, and Vd11 are also somewhat distant from the main groups, and very close to one of the axes, but are clearly separated from group Na-Nb. Strikingly, one member of subgroup Ve (Ve3) is very close to a third group of taxa including all isolates of Vb and Vd except Vb6, Vb9, Vd4, and Vd5. The last four isolates form a clear group centered on the ideal species TV1B and TV1D and close to the main Vb-Vd cluster.

Figure 2 gives the positions of the important molecular (Fig. 2b) and morphological (Fig. 2c) characteristics of the anamorphs that are significant for the characterization of the three main entities including the ideal species that we found: (i) TV1B and TV1D; (ii) TV2A and TV2B; and (iii) ATRO, KONI, and TV1E. With respect to molecular characteristics, we found randomly amplified polymorphic DNA (RAPD) patterns, ITS and 28S rDNA sequences, and RFLP patterns of the endochitinase gene to be group specific. Among the large number of physiological and morphological characteristics, we found that the growth rate on PDA at 30°C, time when conidia developed first on SNA at 25°C, colony radius after 48 h of growth on SNA at 25°C, surface of aggregates on CMD, width of the hypha below each phialide, phialide width, and conidial shape were significant for each of the three groups. We had no

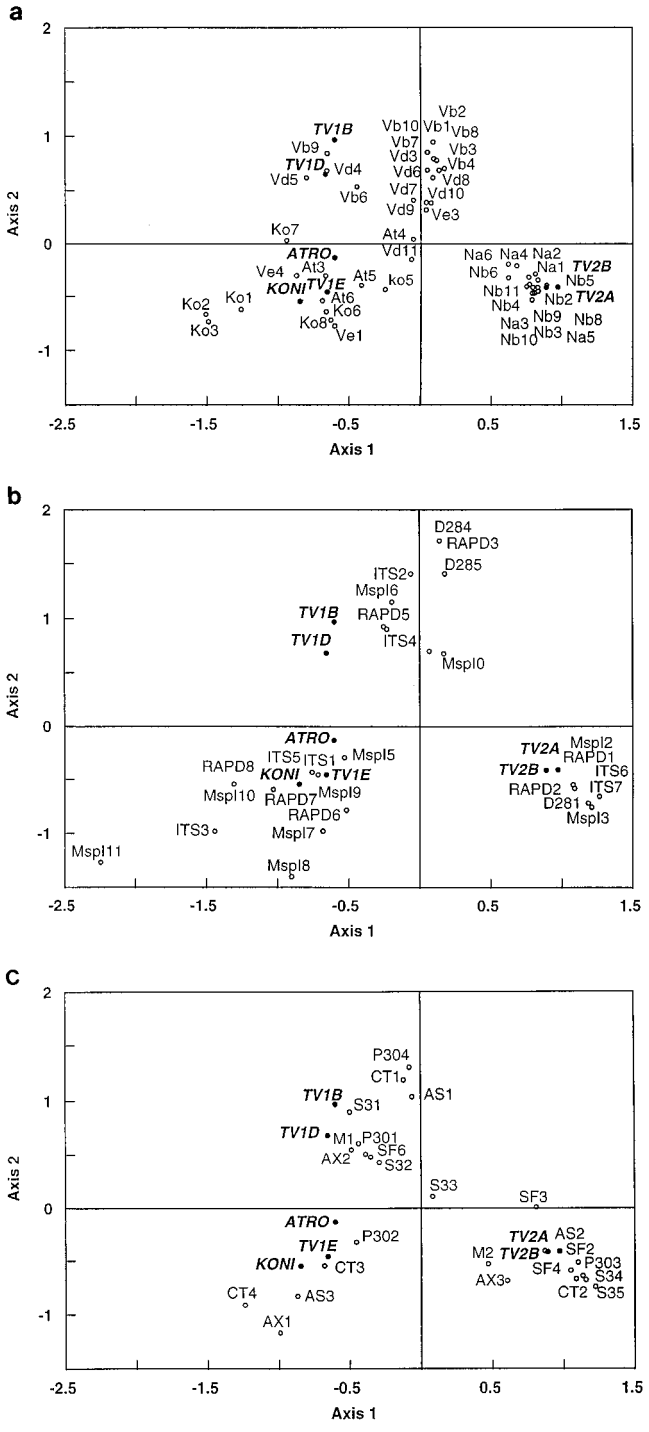

FIG. 2. Discrimination of *T. viride* taxa by simple CA. (a) Graph of all 47 isolates and the ideal species supplemented after the analysis; (b) graph of important molecular characteristics and ideal species; (c) graph of important morphological characteristics of the anamorphs and ideal species. The scales of the two axes in all panels are the same, and the black dots of the ideal species are added to provide orientation.

teleomorph data for the group Na-Nb, but some teleomorph characteristics were useful for the characterization and separation of groups Vb-Vd and At-Ko-Ve from each other.

Biogeography. The strains that we used in this study were obtained from culture collections or were isolated by us. Thus,

the geographic representation of the set of strains is limited. All groups have a cosmopolitan distribution, each including one or more strains that originated from Europe or North America as well as from either eastern Asia or the southwest Pacific region. With regard to types I (Vb and Vd) and II (Na and Nb) of *T. viride*, all strains of type I occurred in northern or southern temperate locations whereas there seemed to be a tendency for strains of type II to occur in warm regions.

DISCUSSION

We have used a polyphasic approach that combines data sets from morphological, physiological, and molecular investigations to study relationships among strains of *T. viride*. Formal, traditional taxonomy is based solely on morphology or, more recently, and alternatively, on molecular data only. Although this has been a major point of criticism by fungal taxonomists (43), there are only a few examples of the use of combined data sets in studies of fungi (34, 35, 45). Perhaps this is due to the complexity of mathematical analyses using mixed types of data. Cluster analysis (used to detect groupings in data) and CA (with the main advantage of obtaining corresponding characteristics and taxon ordination simultaneously) were used in our study to handle the large data sets. Initially, all data were evaluated independently and then combined in a single analysis to find out whether groupings of strains were still supported and to deduce characteristics that are significant for species or group recognition.

The results of DNA sequencing clearly support Meyer's (28) contention that *T. viride* is paraphyletic. The base pair sequence differences between *T. viride* types I and II were in the range of interspecies variability compared to data for other species of the same genus (21, 24). Additional molecular data as well as morphological characteristics unanimously confirm the existence of *T. viride* types I and II, with type I representing Vb and Vd and type II representing Na and Nb. *T. viride* type I (Vb plus Vd) can be distinguished from *T. viride* type II (Na plus Nb) by ITS sequences, PCR fingerprinting patterns, RFLPs of the 42-kDa endochitinase gene, growth rate (especially at 35°C), colony characteristics, branching patterns of conidiophores, morphology of phialides, and conidial ornamentation. These differences indicate that *T. viride* type II is a distinct species, for which we have formally proposed the name *T. asperellum* in another publication (41). Basically, *T. viride* can be recognized under a light microscope by its strongly warted, subglobose to globose conidia.

Meyer's type II accounts for collections that have finely ornamented, subglobose to broadly ellipsoidal conidia. ITS sequencing resolved type II into two groups, which differed from each other by 1 bp each in ITS-1 and ITS-2. In comparison to the ITS sequence variability noted for several species of *Trichoderma* (reviewed in reference 23), this is in the range of intraspecies variation. To test our findings from ITS sequencing (e.g., the possibility of a subgroup splitting in *T. viride* type II), other molecular characteristics were used. The final CA suggests that, according to the molecular data, (i) type II may be considered a separate entity and (ii) subgroups (Na and Nb) are resolved. We could not find, however, any justification morphologically to recognize the groups Na and Nb as independent taxa, and thus in the CA of combined data the subgroups Na and Nb of *T. viride* type II form only a single species (Fig. 2).

T. viride type I is not as straightforward as type II. We found groups that could be readily recognized by conidial morphology, ornamentation, the branching pattern of conidiophores, and phialide morphology. Strikingly, molecular data did not resolve subgroups. This might be due to highly similar ITS sequences: each of the morphologically characterized groups differed from each other by no more than 7 bp, values that are common for intraspecies variation in the genus *Trichoderma* (23).

Our examination of the specimen of *T. viride* from the Persoon herbarium, which Bisby (2) designated the lectotype, shows subglobose conidia that have large, conical warts and are consistent with most of the representatives of *T. viride* type I subgroups Vb and Vd. We agree with Meyer (27, 28) that his *T. viride* type I is true *T. viride*. The Persoon material is too old to show how the phialides are arranged, but a few hooked phialides, typical of *T. viride* type I subgroups Vb and Vd, were seen, and there was an indication of a branching pattern that we described for type I. Unfortunately, we were unable to obtain DNA from conidia of this specimen in two attempts.

ITS sequences of subgroups At and Ko are identical to sequences published by Kuhls et al. (21) for *T. atroviride* and for *T. koningii*/*H. koningii* (24), respectively. Strains of both groups differed from *T. viride* in having smooth conidia that were subglobose (At) or oblong and at most slightly ornamented (Ko).

A number of isolates had a somewhat isolated position in the CA display. In most cases, the small amount of molecular data available for the isolates could be a reason for the positions of the isolates in the graph (At4, Vd11, and Ko7). The position of Ve3 close to Vb and Vd is supported by morphological and most of the molecular data, except the ITS-1 sequence, which strongly differs from the types found for Vb and Vd. The three isolates Ko1, Ko2, and Ko3 were all *Hypocrea* strains collected in Taiwan; morphologically, they fit the description of *H. vinosa*. In Fig. 2a, a slight splitting of strains of subgroups Vb and Vd is visible. Interestingly, the four strains (Vb6, Vb9, Vd4, and Vd5) that are closest to the ideal species TV1B and TV1D are all anamorphs of *H. rufa* collections, whereas the main and very large group of Vb and Vd represents only *T. viride* collections. This last interpretation, however, must be taken with caution, since the distances on the map barely allow one to draw firm conclusions. The findings, however, do not contradict the general outcome of the CA of morphological, physiological, and molecular characteristics with respect to the characterization of two species of *T. viride*. In ongoing experiments, emphasis is on a detailed characterization of the relationship between the true *T. viride*—subgroups Vb and Vd, *T. atroviride*, and *T. koningii*—and the more diverse group Ve by extending the number of *Trichoderma* and *Hypocrea* strains that morphologically fit into this complex. We have checked the possibility that group Ve is similar or even identical to *T. pubescens* or *T. strigosum*, both of which have been shown recently to cluster near *T. viride* (16). We have also tested whether Ve could be one of the *Hypocrea* sp. cf. *muroiana* sequence types that have been described previously (24). In all sequence comparisons so far, strains of Ve remained a separate cluster, but it must be emphasized again that the level of genetic variability in the genus *Trichoderma*, as concluded from molecular data, is very low. The results of the extended investigations will perhaps answer the question of whether all strains that we studied and that exhibit a low level of genetic diversity and intergrading phenotypic characteristics should be recognized as distinct taxa on some level. The high degree of genetic similarity of species within section *Trichoderma* with overlapping sequence variation in ITS-1 and ITS-2 of the rDNA nicely reflects the processes of evolution and speciation.

The teleomorphs encountered in this study are phenotypically homogeneous. We detected small differences in ascospore measurements, but while these differences were statisti-

cally significant, their biological significance is doubtful. These collections agree in most details with the description of *H. rufa* that was published by Webster (50). The main differences are that Webster reported larger ascospores (distal, 5.5 to 7.2 by 4.5 to 5.0 μm; proximal, 5.5 to 7.0 by 3.6 to 4.5 μm) for one of his English specimens than we have observed (3.9 to 5.3 by 4.1 to 4.6 μm and 4.1 to 5.7 by 3.0 to 4.2 μm, respectively). Other specimens listed by Webster had smaller ascospores. The anamorph reported by Webster as *T. viride* fits in with our concept of *T. viride* but produced abundant chlamydospores.

The cosmopolitan distribution of *Trichoderma* species makes them ideal candidates for biocontrol applications in different habitats, but the sensitivity of single strains to abiotic environmental factors must be considered (15). Köhl and Schlösser (17) reported differences in antagonistic activity at different temperatures among *Trichoderma* isolates within a species group. Temperature tolerance of biocontrol isolates relative to that of the pathogen could be critical to the success of an application. Because *T. viride* is often cited as producing antibiotics and as acting as a fungal antagonist and potential biocontrol agent against soilborne plant-pathogenic fungi (1, 38), it was especially interesting and important to learn about the temperature optimum of *T. viride* type I and II strains. Types I and II of *T. viride* are easily separated on the basis of temperature optima. Type II (*T. asperellum*) has an optimum of 30°C and a maximum of >35°C, and true *T. viride* has an optimum temperature of 22.5°C and a maximum of 30°C. The temperature tolerance of strains might be an important factor with respect to *T. viride* strains that act as promoters or inhibitors of plant growth (25, 26) or even as weed pathogens in mushroom cultures (42). The strikingly different temperature optima among *T. viride* strains was also noted by Fujimori and Okuda (8), who described two groups clearly separated by RAPD analysis. Furthermore, both groups were characterized as producers or nonproducers of isonitrile antibiotics. We have analyzed representatives of both groups morphologically and by RFLP analysis of the ITS-1–5.8S–ITS-2 rDNA region and the endochitinase gene. *T. viride* NR 5566 and NR 6937 (isonitrile antibiotic producers) are strains of *T. asperellum*, the new species, whereas NR 5510, NR 5541, NR 6898, NR 6955, NR 6896, NR 6969, FP 5563, and FP 5564 (nonproducers) are true *T. viride*.

Of the strains that we originally investigated, only Tr48 has been used in published physiological or biocontrol studies (14); we have investigated a larger number of *T. viride* strains with biocontrol application listed in the American Type Culture Collection catalogue (ATCC 20900, ATCC 20905, ATCC 90200, ATCC 34650, ATCC 38717, and ATCC 52439). Only one of the six strains had finely warted conidia and was identified as *T. asperellum*. The remaining five strains have molecular characters similar to those of members of *Trichoderma* section *Pachybasium*, which includes *T. inhamatum* and *T. harzianum*. In a list of commercial biocontrol products for use against soilborne crop diseases (47a), we found only one *T. viride* strain. We have analyzed the substratum Ecofit in terms of isolating DNA from conidia as well as from mycelium of the included fungus. The fungus was identified as *T. asperellum*, too. In a search of sequence data banks, we found two *T. harzianum* strains used in biocontrol which have the same sequence types as subgroup a of type II, viz. *T. harzianum* T-203 (accession no. AF04971 [3a]) and *T. harzianum* strain 3 (accession no. Y13575 [12]). Moreover, a number of sequences submitted for strains identified as *T. viride* that have biocontrol activities are actually *T. asperellum* (accession no. AF059515 (4). In several cases, the strains were *T. atroviride* (ATCC 32173 [30]; DB 35916, IMI 296237, and IMI 304531 [1]; and IMI 110150 [12]). All search results strongly indicate that *T. viride* biocontrol strains reported to have high temperature optima are actually *T. asperellum*. No true *T. viride* strain was found to produce antibiotics.

ACKNOWLEDGMENTS

This work was supported by grant EL 627/4 from the Deutsche Forschungsgemeinschaft (Bonn, Germany) to E.L. and by a grant from the Fond der Chemischen Industrie (Frankfurt am Main, Germany) to Thomas Börner (Humboldt-Universität, Berlin, Germany). G.J.S. was supported in part by NSF-97-12308 (a PEET grant) to the Pennsylvania State University.

We are grateful to R. Vilgalys and T. G. Mitchell (Duke University, Durham, N.C.) for providing the rDNA primers. We also thank B. Liebe, Y. Claußner, and Yolaine Covignac (Berlin) for technical assistance; J. Müller (Berlin) for sequencing with the automatic sequencer; and J. Plaskowitz (USDA-ARS, Beltsville, Md.) for preparing the SEM samples.

REFERENCES

1. **Arisan-Atac, I., E. Heidenreich, and C. P. Kubicek.** 1995. Randomly amplified polymorphic DNA fingerprinting identifies subgroups of *Trichoderma viride* and other *Trichoderma* sp. capable of chestnut blight biocontrol. FEMS Microbiol. Lett. **126:**249–256.
2. **Bisby, G. R.** 1939. *Trichoderma viride* Pers. ex Fries, and notes on *Hypocrea*. Trans. Br. Mycol. Soc. **23:**149–168.
3. **Chet, I.** 1987. *Trichoderma*—application, mode of action, and potential as biocontrol agent of soilborne plant pathogenic fungi, p. 137–160. *In* I. Chet (ed.), Innovative approaches to plant disease control. John Wiley & Sons, New York, N.Y.

3a. **Chet, I.** 1998. Personal communication.

4. **Dodd, S., R. N. Crowhurst, A. G. Rodrigo, G. J. Samuels, R. A. Hill, and A. Stewart.** Examination of *Trichoderma* phylogenies derived from ribosomal DNA sequence data. Mycol. Res., in press.
5. **Domsch, K. H., W. Gams, and T.-H. Anderson.** 1980. Compendium of soil fungi, vol. 1 Academic Press, London, United Kingdom.
6. **Fekete, C. T. Weszely, and L. Hornok.** 1996. Assignment of a PCR-amplified chitinase sequence cloned from *Trichoderma hamatum* to resolved chromosomes of potential biocontrol species of *Trichoderma*. FEMS Microbiol. Lett. **145:**385–391.
7. **Felsenstein, J.** 1985. Confidence limits on phylogenies: an approach using the bootstrap. Evolution **39:**783–791.
8. **Fujimori, F., and T. Okuda.** 1994. Application of the random amplified polymorphic DNA using the polymerase chain reaction for efficient elimination of duplicate strains in microbial screening. I. Fungi. J. Antibiot. **47:**173–182.
9. **Gams, W., and W. Meyer.** 1998. What exactly is *Trichoderma harzianum* Rifai? Mycologia **90:**904–915.
10. **Greenacre, M. J.** 1986. SimCA: a program to perform simple correspondence analysis. Am. Stat. **40:**230–231.
11. **Greenacre, M. J.** 1992. Correspondence analysis in medical research. Stat. Methods Med. Res. **1:**97–117.
12. **Grondona, I., R. Hermosa, M. Tejada, M. D. Gomis, P. F. Mateos, P. D. Bridge, E. Monte, and I. Garcia-Acha.** 1997. Physiological and biochemical characterization of *Trichoderma harzianum*, a biological control agent against soilborne fungal plant pathogens. Appl. Environ. Microbiol. **63:**3189–3198.
13. **Gueho, E., L. Improvis, R. Christen, and G. S. De Hoog.** 1993. Phylogenetic relationships of *Cryptococcus neoformans* and some related basidiomycetous yeasts determined from partial large subunit rRNA sequences. Antonie Leewenhoek **63:**175–189.
14. **Hau, C. T., A. Ciegler, and C. W. Hesseltine.** 1972. New mycotoxin, a trichotoxin from *Trichoderma viride* isolated from southern leaf blight-infected corn. Appl. Microbiol. **23:**183–185.
15. **Hjeljord, L., and A. Tronsmo.** 1998. *Trichoderma* and *Gliocladium* in biocontrol: an overview, p. 131–151. *In* C. P. Kubicek and G. E. Harman (ed.), *Trichoderma* and *Gliocladium*. Taylor & Francis Ltd., London, United Kingdom.
16. **Kindermann, J., Y. El-Ayouti, G. J. Samuels, and C. P. Kubicek.** 1998. Phylogeny of the genus *Trichoderma* based on sequence analysis of the internal transcribed spacer 1 of the rDNA cluster. Fungal Genet. Biol. **24:**298–309.
17. **Köhl, J., and E. Schlösser.** 1989. Decay of sclerotia of *Botrytis cinerea* by *Trichoderma* spp. at low temperatures. J. Phytopathol. **125:**320–326.
18. **Kornerup, A., and J. H. Wanscher.** 1978. Methuen handbook of colour. Methuen, London, United Kingdom.
19. **Kuhls, K., E. Lieckfeldt, and T. Börner.** 1995. PCR-fingerprinting used for comparison of ex type strains of *Trichoderma* species deposited in different

culture collections. Microbiol. Res. **150:**363–371.
20. **Kuhls, K., E. Lieckfeldt, G. J. Samuels, W. Kovacs, W. Meyer, O. Petrini, W. Gams, T. Börner, and C. P. Kubicek.** 1996. Molecular evidence that the asexual industrial fungus *Trichoderma reesei* is a clonal derivative of the ascomycete *Hypocrea jecorina*. Proc. Natl. Acad. Sci. USA **93:**7755–7760.
21. **Kuhls, K., E. Lieckfeldt, G. J. Samuels, W. Meyer, C. P. Kubicek, and T. Börner.** 1997. Revision of *Trichoderma* sect. *Longibrachiatum* including related teleomorphs based on analysis of ribosomal DNA internal transcribed spacer sequences. Mycologia **89:**442–460.
22. **Leuchtmann, A., O. Petrini, and G. J. Samuels.** 1996. Isozyme subgroups in *Trichoderma* section *Longibrachiatum*. Mycologia **88:**384–394.
23. **Lieckfeldt, E., K. Kuhls, and S. Muthumeenakshi.** 1998. Molecular taxonomy of *Trichoderma* and *Gliocladium* and their teleomorphs, p. 35–56. *In* C. P. Kubicek and G. E. Harman (ed.), *Trichoderma* and *Gliocladium*. Taylor & Francis Ltd., London, United Kingdom.
24. **Lieckfeldt, E., G. J. Samuels, T. Börner, and W. Gams.** 1998. *Trichoderma koningii*: neotypification and *Hypocrea* teleomorph. Can. J. Bot. **76:**1507–1522.
25. **Lindsey, D. L., and R. Baker.** 1967. Effect of certain fungi on dwarf tomatoes grown under gnotobiotic conditions. Phytopathology **57:**1262–1263.
26. **Menzies, J. G.** 1993. A strain of *Trichoderma viride* pathogenic to germinating seedlings of cucumber, pepper and tomato. Plant Pathol. **42:**784–791.
27. **Meyer, R., and J. S. Plaskowitz.** 1989. Scanning electron microscopy of conidia and conidial matrix of *Trichoderma*. Mycologia **81:**312–317.
28. **Meyer, R. J.** 1991. Mitochondrial DNAs and plasmids as taxonomic characteristics in *Trichoderma viride*. Appl. Environ. Microbiol. **57:**2269–2276.
29. **Meyer, W., R. Morawetz, T. Börner, and C. P. Kubicek.** 1992. The use of DNA-fingerprint analysis in the classification of some species of the *Trichoderma* aggregate. Curr. Genet. **21:**27–30.
30. **Neethling, D., and H. Nevalainen.** 1995. Mycoparasitic species of *Trichoderma* produce lectins. Can. J. Microbiol. **42:**141–146.
31. **Nirenberg, H. I.** 1976. Untersuchungen über die morphologische und biologische Differenzierung inder *Fusarium*-Sektion *Liseola*. Mitt. Biol. Bundesanst. Land- Forstwirtsch. Berl.-Dahl. **169:**1–117.
32. **Papavizas, G. C.** 1985. *Trichoderma* and *Gliocladium*: biology, ecology, and potential for biocontrol. Annu. Rev. Phytopathol. **23:**23–54.
33. **Persoon, C. H.** 1794. Dispositio methodica fungorum. Römer's neues Bot. Mag. **1:**81–128.
34. **Petrini, L. E.** 1992. *Rosellinia* species of the temperate zones. Sydowia **44:** 169–281.
35. **Petrini, O., L. E. Petrini, G. Laflamme, and G. B. Oulette.** 1989. Taxonomic position of *Gremmeniella abietina* and related species: a reappraisal. Can. J. Bot. **67:**2805–2814.
36. **Rifai, M. A.** 1969. A revision of the genus *Trichoderma*. Mycol. Papers **116:**1–56.
37. **Sambrook, J., E. F. Fritsch, and T. Maniatis.** 1989. Molecular cloning: a laboratory manual, 2nd ed. Cold Spring Harbor Laboratory, Cold Spring Harbor, New York.
38. **Samuels, G. J.** 1996. *Trichoderma*: a review of biology and systematics of the genus. Mycol. Res. **100:**923–935.
39. **Samuels, G. J., O. Petrini, and S. Manguin.** 1994. Morphological and macromolecular characterization of *Hypocrea schweinitzii* and its *Trichoderma* anamorph. Mycologia **86:**421–435.
40. **Samuels, G. J., O. Petrini, K. Kuhls, E. Lieckfeldt, and C. P. Kubicek.** 1998. The *Hypocrea schweinitzii* complex and *Trichoderma* sect. *Longibrachiatum*. Stud. Mycol. **41:**1–54.
41. **Samuels, G. J., E. Lieckfeldt, and H. I. Nirenberg.** 1999. Description of *T. asperellum* sp. nov. and comparison to *T. viride*. Sydowia **51:**71–88.
42. **Seaby, D.** 1998. *Trichoderma* as a weed mould or pathogen in mushroom cultivation, p. 267–288. *In* C. P. Kubicek and G. E. Harman (ed.), *Trichoderma* and *Gliocladium*. Taylor & Francis Ltd., London, United Kingdom.
43. **Seifert, K. A., B. D. Wingfield, and M. J. Wingfield.** 1995. A critique of DNA sequence analysis in the taxonomy of filamentous *Ascomycetes* and ascomycetous anamorphs. Can. J. Bot. **73**(Suppl. 1)**:**S760–S767.
44. **Sieber, T. N., O. Petrini, and M. J. Greenacre.** 1998. Correspondence analysis as a tool in fungal taxonomy. Syst. Appl. Microbiol. **21:**442–449.
45. **Sieber-Canavesi, F., O. Petrini, and T. N. Sieber.** 1991. Endophytic *Leptostroma* species on *Piecea abies*, *Abies alba*, and *Abies balsamea*: a cultural, biochemical, and numerical study. Mycologia **83:**89–96.
46. **Swofford, D. L.** 1993. PAUP, Phylogenetic Analysis Using Parsimony, version 3.1.1. Computer program distributed by the Illinois Natural History Survey, Champaign.
47. **Turner, D., W. Kovacs, K. Kuhls, E. Lieckfeldt, B. Peter, L. Arisan-Atac, J. Strauss, G. J. Samuels, T. Börner, and C. P. Kubicek.** 1997. RAPD-analysis of world-wide distribution and genetic variation of *Trichoderma* spp. and *Hypocrea schweinitzii* (Fr.:Fr.) Sacc. belonging to *Trichoderma* section *Longibrachiatum*. Mycol. Res. **101:**449–459.
47a. **USDA, Beltsville Agricultural Research Center.** 1999. Commercial biocontrol products for use against soilborne crop diseases. [Online.] http://www.barc.usda.gov/psi/bpdl/bioproduct/htm. [23 April 1999, date last accessed.]
48. **van de Peer, Y.** 1994. User manual for Treecon, version 3.0, a software package for the construction and drawing of evolutionary trees. University of Antwerp, Antwerp, Belgium.
49. **Vilgalys, R., and M. Hester.** 1990. Rapid genetic identification and mapping of enzymatically amplified ribosomal DNA from several *Cryptococcus* species. J. Bacteriol. **172:**4238–4246.
50. **Webster, J.** 1964. Culture studies on *Hypocrea* and *Trichoderma*. I. Comparison of perfect and imperfect states of *H. gelatinosa*, *H. rufa*, and *Hypocrea* sp. 1. Trans. Br. Mycol. Soc. **47:**75–96.
51. **Wilkinson, L.** 1996. Systat 6.0 for Windows: statistics. SPSS Inc., Chicago, Ill.